Inhibition of Topoisomerase II Catalytic Activity by Two Ruthenium Compounds: A Ligand-Dependent Mode of Action†

Y. N. Vashisht Gopal, D. Jayaraju, and Anand K. Kondapi*

Department of Biochemistry, School of Life Sciences, University of Hyderabad, Hyderabad-46, India

Received August 18, 1998; Revised Manuscript Received January 7, 1999

ABSTRACT: The ability of two structurally different ruthenium complexes to interfere with the catalytic activity of topoisomerase II was studied to elucidate their molecular mechanism of action and relative antineoplastic activity. The first complex, $[RuCl_2(C_6H_6)(dmso)]$, could completely inhibit DNA relaxation activity of topoisomerase II and form a drug-induced cleavage complex. This strongly suggests that the drug interferes with topoisomerase II activity by cleavage complex formation. The bi-directional binding of $[RuCl_2(C_6H_6)(dmso)]$ to DNA and topoisomerase II was verified by immunoprecipitation experiments which confirmed the presence of DNA and ruthenium in the cleavage complex. The second complex, Ruthenium Salicylaldoxime, could not inhibit topoisomerase II relaxation activity appreciably and also could not induce cleavage complex formation, though its DNA-binding characteristics and antiproliferation activity were almost comparable to those of $[RuCl_2(C_6H_6)(dmso)]$. The results suggest that the difference in ligands and their orientation around a metal atom may be responsible for topoisomerase II poisoning by the first complex and not by the second. A probable mechanism is proposed for $[RuCl_2(C_6H_6)(dmso)]$, where the ruthenium atom interacts with DNA and ligands of the metal atom form cross-links with topoisomerase II. This may facilitate the formation of a drug-induced cleavage complex.

Type II topoisomerases are a class of ubiquitous enzymes essential for maintaining genome organization in the dense nuclear milieu of eukaryotic cells (*1*, *2*). Topoisomerase II (topo II)[1] plays an important role in replication, transcription, recombination, and segregation of chromosome pairs during cell division (*3*, *4*). It is also involved in maintaining the structural organization of the mitotic chromosomal scaffold (*5*−*7*). The enzyme assists in these functions by altering the topological properties of DNA, which it catalyzes by creating transient double strand breaks, transporting an intact segment of DNA through the gap and finally religating the cleaved strands (*8*−*11*). Topo II is present as a major enzyme in the nuclei of rapidly dividing cells, especially in neoplastic conditions (*2*). During the past decade, numerous studies have indicated that selective poisoning of this enzyme leads to effective inhibition of neoplastic cell proliferation (*8*, *12*, *13*). A number of clinically prescribed anticancer drugs are now known to be topo II poisons. Topo II poisons are broadly classified into two types: (1) cleavable complex-forming compounds (DNA intercalating, e.g., m-AMSA, nonintercalating e.g., Etoposide) and (2) Noncleavable complex-forming compounds (e.g. ICRF-193) (*8*, *14*, *15*). Cleavage complex-forming compounds are of particular interest because they shift the enzyme's cleavage/religation cycle toward DNA cleavage and form a stable drug-mediated enzyme-cleaved DNA complex (*16*).

Metal complexes gained immense importance with the discovery of cisplatin as an anticancer agent in 1969. Since then, numerous complexes of metals of the main group, early transition, and late transition series of the periodic table have been vigorously tested for anticancer activity. However, very few of them have qualified for phase I and phase II clinical trials (*18*). Among the metal atoms used in anticancer metal complexes, ruthenium is most unique. It is a rare noble metal unknown to living systems and has a strong complex-forming ability with numerous ligands. In vitro and in vivo studies reveal that most ruthenium complexes bind covalently to DNA via the N-7 atom of purines and cause cytotoxicity by possibly inhibiting cellular DNA synthesis (*18*, *19*). Ruthenium complexes have a stronger affinity for cancer tissues than normal tissues. This is because ruthenium binds readily to transferrin molecules in plasma and is transported to the tumor tissues. Here, the ruthenium−transferrin complex is internalized into tumor cells through transferrin receptors which are abundantly expressed on the surface of tumor cells (*20*). Ruthenium(III) complexes have been hypothesized to function as pro-drugs which are reduced to the more reactive ruthenium(II). In this state, they coordinate with biological macromolecules and induce toxicity (*20*).

In the present study, we have examined and compared two structurally different ruthenium(II) complexes for their antiproliferation activity and molecular action on topo II to determine their efficacy as anticancer agents and their molecular mechanism of action.

MATERIALS AND METHODS

Materials. Topo II was purified from rat liver following the procedure of Galande et al. (*21*). The enzyme concentration was determined using Bradford colorimetric assay (*22*). The negatively supercoiled pBR322 plasmid DNA was

† This work was supported by the Council of Scientific and Industrial Research, India, Sanction number: 37 (0854)/93/EMR-II.

* To whom correspondence should be addressed. Tel: 91-40-3010 500, ext. 4571. Fax: 91-40-3010 120 or 145. E-mail: akksl@uohyd.ernet.in.

[1] Abbreviations: RuBen, $[RuCl_2(C_6H_6)(dmso)]$; RuSal, ruthenium salicylaldoxime; m-AMSA, 4-[9-acridinylamino]-*N*-[methanesulfonyl]-*m*-anisidine; topo II, topoisomerase II; SDS, sodium dodecyl sulfate; DTT, dithiothreitol.

10.1021/bi981990s CCC: $18.00
Published on Web 03/16/1999

purified as described by Wang and Rossman (*23*). Anti-topoisomerase II antibody was from Topogen Inc.; RPMI-1640 medium, m-AMSA, and calf thymus DNA were from Sigma Chemical Co.; protein A agarose, fetal calf serum, and antibiotics were from Gibco-BRL; PEI (polyethyleneimine) Cellulose-F TLC sheets were from Merck; Proteinase K and ATP were from Boehringer-Mannheim; and γ^{32}P−ATP and ^{3}H-labeled thymidine were supplied by BRIT, India. Other chemicals and biochemicals were of analytical grade.

Synthesis of the Ruthenium Complexes. (a) RuBen ([$RuCl_2(C_6H_6)$(dmso)]). This was synthesized following the procedure of Zelonka and Baird (*24*). Freshly synthesized 1,3-hexadiene (6 mL) was added to $RuCl_3 \cdot 3H_2O$ (1.7 g) in 100 mL of 90% aqueous ethanol. The solution was heated at 45 °C for 3 h to form a red precipitate, which was washed in ethanol and dried in vacuo to give the dimeric complex $[RuCl_2(C_6H_6)]_2$. To this dimer, DMSO was added to form the monomeric DMSO complex $[RuCl_2(C_6H_6)$(dmso)] and vacuum-dried. *NMR spectra in d_6-DMSO: δ 4.07 ppm (identical with that reported by Zelonka and Baird).*

(b) RuSal (Trans bis salicylaldoximato ruthenium (II)). This was synthesized following a slightly modified procedure of Lumme et al. (*25*) for the synthesis of copper salicylaldoxime. Dry salicylaldoxime (10 mmol) was dissolved in dry methanol, and anhydrous ruthenium trichloride (5 mmol) was added in the presence of dry nitrogen gas. The constituents were refluxed at 70 °C for about 1 h until a green solution formed. This was vacuum-dried and crystallized to form dark green complex of ruthenium (II) salicylaldoxime. *IR spectra: Band at 1608 cm^{-1} confirms the formation of a coordination bond between imine nitrogen and metal atom; band at 1493 cm^{-1} confirms the metal−oxygen bond.*

Molecular Modeling and Energy Minimization. The atomic coordinates for RuBen and RuSal were generated employing standard geometry and then refined using the energy minimization procedure of Vinter et al. (*35*) at all atom levels on Desktop Molecular Modeler software (distributed by Oxford University Press) (Figure 1). In RuBen, the organometallic bond between the ruthenium atom and benzene was simulated on the basis of the information obtained from literature (*36*).

Solubilization of Complexes. The ruthenium complexes and m-AMSA were dissolved in DMSO and diluted with deionized water prior to use in the biological assays. All of the DNA and topo II controls in our experiments contained 1% DMSO, which was equivalent to the maximum amount of DMSO present in the drug-containing assay samples. DMSO at this concentration had no effect on the assays.

In vitro Antiproliferation Activity. ^{3}H-Thymidine incorporation assays were performed to analyze the effect of the ruthenium complexes on the proliferative response of cancer cells. Crit-2 (nonhodkins human lymphoma) cells were grown in RPMI-1640 medium supplemented with 10% fetal calf serum. Cells (0.2×10^6/200 μL) were distributed in triplicates in a 96-well microtiter tissue culture plate. The cultures were incubated for 16 h at 37 °C in a CO_2 incubator maintaining 5% CO_2 atmosphere. The two ruthenium drugs were added to the cells at increasing concentrations (negative controls contained an equivalent amount of DMSO present in the drug-treated samples). After further incubation for 8 h, the cultures were pulsed with 0.5 μCi of ^{3}H-thymidine.

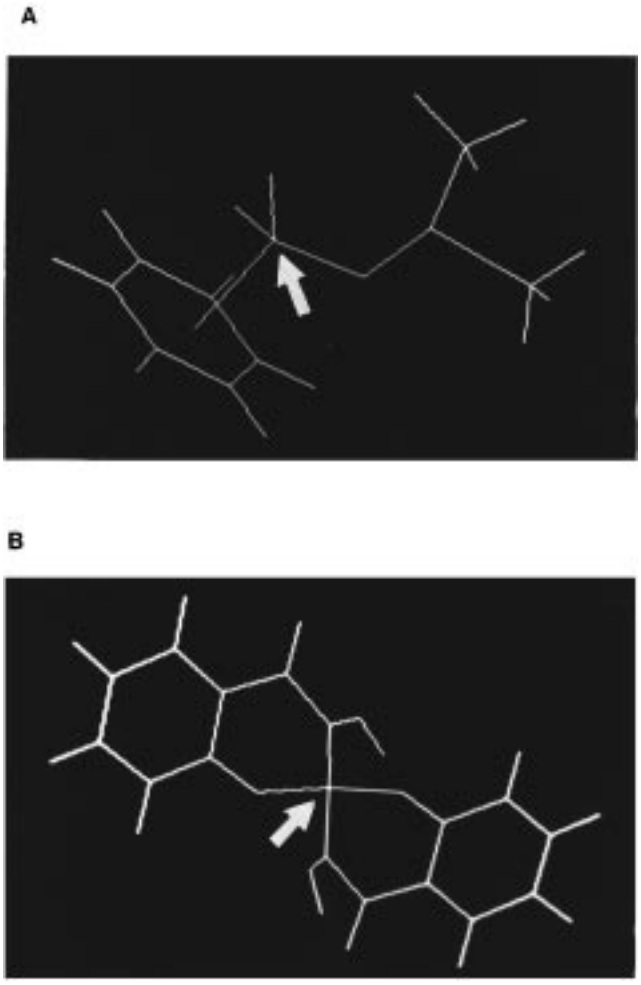

FIGURE 1: Three-dimensional chemical structures of RuBen (A) and RuSal (B) represented as line diagrams. The arrows point toward the ruthenium atom.

Incubation was continued for 4 h to allow thymidine incorporation by cells. The cells were harvested on glass microfiber strips using a Skatron automated cell harvester. Radioactivity was measured in a Wallac liquid scintillation counter.

Relaxation Assay. This assay was performed following the procedure of Osheroff et al. (*26*). The reaction mixture (20 μL) contained relaxation buffer (50 mM Tris-HCl (pH 8.0), 120 mM KCl, 0.5 mM EDTA, 0.5 mM DTT, 10 mM $MgCl_2$, 30 μg/mL BSA, 1 mM ATP), 0.6 μg of negatively supercoiled pBR322 plasmid DNA (>95% supercoiled), and increasing concentrations of the ruthenium drugs. The reaction was initiated by adding 2 units (~8 nM) of topo II, and the mixture was incubated at 30 °C for 15 min. The reaction was stopped by the addition of 2 μL of 10% SDS. To this, 3 μL of loading dye (0.5% bromo-phenol blue, 0.5% xylene cyanol, 60% sucrose, 10 mM tris-HCl, pH 8.0) was added, and the products were separated on a 1% agarose gel in 0.5× TAE buffer (20 mM tris-acetate, 0.5 mM EDTA) at 50 V for 12 h. The gel was stained with ethidium bromide, visualized in a Photodyne UV transilluminator, and photographed.

Cleavage Assay. The formation of the cleavage complex was assayed following the procedure of Zechiedrich et al. (*27*). The 20 μL reaction mixture contained relaxation buffer (minus ATP), 0.6 μg of pBR322 supercoiled DNA (70%

supercoiled, 30% nicked circular), and increasing concentrations of drugs. The reaction was initiated by adding 10 units (40 nM) of topoisomerase II and incubated at 30 °C for 15 min. The reaction was stopped with 2 μL of 10% SDS. The DNA-bound protein was degraded by incubating the reaction mixture with 2 μL of 1 mg/mL Proteinase K at 45 °C for 1 h. The products were separated on 1% agarose gel for 8 h at 50 V in 1× TAE buffer (40 mM tris-acetate, 1 mM EDTA), stained, and photographed. The linear DNA band was quantified as a percentage of total DNA in a UVP gel documentation system.

ATPase Activity Assay. This assay is a modified procedure of Osheroff et al. (*26*). The 20 μL reaction mixture contained relaxation buffer (the 1 mM ATP component contained 0.025 μCi γP^{32}-ATP), 0.6 μg of pBR322 DNA, and increasing concentrations of drugs. The reaction was initiated with 2 units of topo II and incubated at 30 °C for 15 min. The reaction was stopped with 2 μL of 250 mM EDTA. The reaction mixture was spotted on PEI cellulose-F TLC sheets, and the sheets were subjected to thin-layer chromatography in 1 M lithium chloride solution. In these conditions, γ^{32} P_i migrates first followed by ADP and γ^{32}P-ATP. After resolution, the bands were monitored under reflected UV light at 366 nm in a Photodyne transilluminator. The illuminated bands of ATP, ADP, and P_i (inorganic phosphate) were cut and counted for ^{32}P in a liquid scintillation counter.

Assay for Ruthenium and DNA in Cleavage Complex. The cleavage assay was performed in the presence of 500 μM ruthenium drugs. After the reaction, topo II in the cleavage complex and in free form was immunoprecipitated with 0.04 units of anti-topo II antibody. The antibody−antigen complex was trapped in 20 μL of protein A agarose. This was washed twice with 1× relaxation buffer at 1000 rpm to remove unbound reactants. Topo II in the immunoprecipitate was released by adding 20 μL of 1% trichloro acetic acid (TCA). To this was added 10 μL of 1 N HCl, and the samples were boiled in steam to dryness. Samples were then analyzed for parts per million of ruthenium metal by atomic absorption spectroscopy in an ECIL-AAS4129 atomic absorption spectrometer. The same assay was performed with ^{3}H-thymidine-labeled DNA. After TCA treatment, the samples were spotted on filter paper strips and the radioactivity was measured.

Drug−DNA Interaction. (a) Thermal Denaturation. Calf thymus DNA (sodium salt) was dissolved in 1 mM sodium phosphate buffer containing 1 mM sodium chloride. The DNA concentration was adjusted to give an absorbance of 1.0 in 1 mL at 260 nm. The ruthenium drugs were added to DNA at concentrations which gave drug-to-nucleotide ratios of 1:20, 1:10, 1:5, 1:2, and 1:1, respectively. The samples were incubated in 1 mL quartz cuvettes for 2 min to allow drug−DNA binding. A Hitachi 150-20 spectrophotometer was set to give a 1 °C rise in temperature per minute with a KPC-6 thermo-programmer and SPR-7 temperature controller. The increase in absorbance at 260 nm was recorded from 40 to 90 °C. T_m was determined from the denaturation curves. The curve width of the individual melting curves was calculated by the procedure of Kelly et al. (*28*). Curve width is the temperature range between which 10−90% of the absorbance increase occurs. The data were plotted and analyzed.

(b) 1D Gel Mobility Assay. pBR322 DNA (0.6 μg) was incubated in increasing concentrations of the drugs in relaxation buffer at 30 °C for 15 min. Loading dye was added and the products were run on a 0.8% agarose gel for 15 h at 25 V in 0.5× TAE buffer.

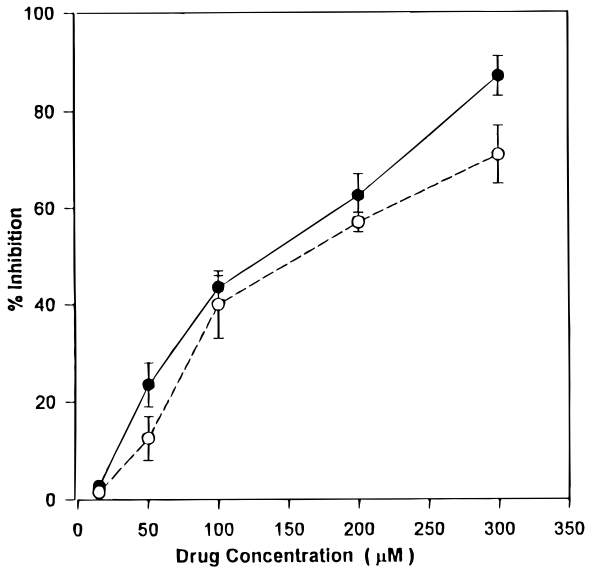

FIGURE 2: Crit-2 cells were incubated with increasing concentrations of RuBen and RuSal. ^{3}H thymidine incorporation during the last 4 h of incubation was measured as described in methods. Values are presented as means of three independent experiments. Data are graphically expressed as a percentage increase in inhibition versus concentration of RuBen (○) and RuSal (●) in micromolar units.

2D Gel Mobility Assay. pBR322 DNA (0.6 μg) was incubated as above in 500 μM ruthenium drugs. The samples were loaded on 0.7% agarose gels and run in the first dimension at 30 V for 10 h in 0.5× TAE buffer. The second dimension was run in similar conditions in the presence of Chloroquine diphosphate (0.5 μg/mL). The gels were documented as in relaxation assay.

(c) CD Spectra. Circular dichroic spectra of pBR322 DNA in the presence of RuBen or RuSal was measured in a Jasco J-715 spectropolarimeter. The DNA and drug concentrations corresponded to 0.6 μg of DNA and 500 μM drug as used in the topoisomerase II catalytic assays. m-AMSA (corresponding to 100 μM concentration in the catalytic assays) was included as a positive control. The spectra were measured in a quartz cuvette of 1 cm path length. Data were represented graphically as molar ellipticity ($[\theta] \times 10^{-3}$ deg cm^{-2}/dmol) versus wavelength (nanometers).

RESULTS

Antiproliferation Activity. Antiproliferation activity of the ruthenium drugs was measured by thymidine incorporation assays. The results show a dose-dependent inhibition of the Crit-2 cell proliferation. At the highest concentration of 300 μM, RuBen inhibited 87% of cell growth, while RuSal showed a marginally less inhibition of 71% (Figure 2).

Relaxation Assay. DNA relaxation activity of topo II in the presence of increasing concentrations of RuBen was significantly inhibited, and at 500 μM, the drug could completely inhibit topo II-catalyzed relaxation of supercoiled pBR322 DNA (Figure 3A). RuSal could partially inhibit the relaxation activity with no significant increase in inhibition up to 500 μM (Figure 3B).

Cleavage Assay. The ability of RuBen and RuSal to cause drug-induced stabilization of DNA-topo II complex was

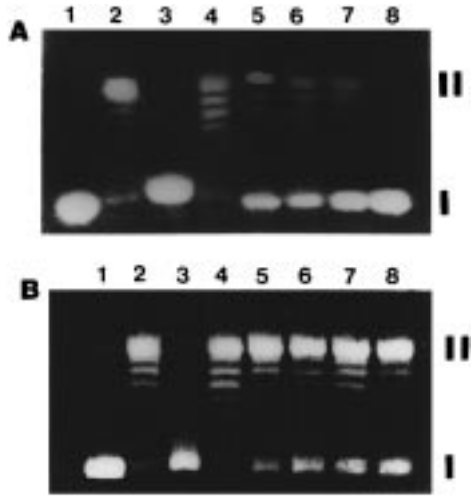

FIGURE 3: Effect of RuBen (A) and RuSal (B) on topo II-catalyzed DNA relaxation activity. Supercoiled pBR322 DNA (lane 1) was incubated with topo II in the absence (lane 2) or presence of 100 μM m-AMSA (lane 3) and 100, 200, 300, 400, and 500 μM ruthenium drugs (lanes 4−8). The positions of supercoiled (form 1) and nicked circular (form 2) DNA are indicated by **I** and **II**.

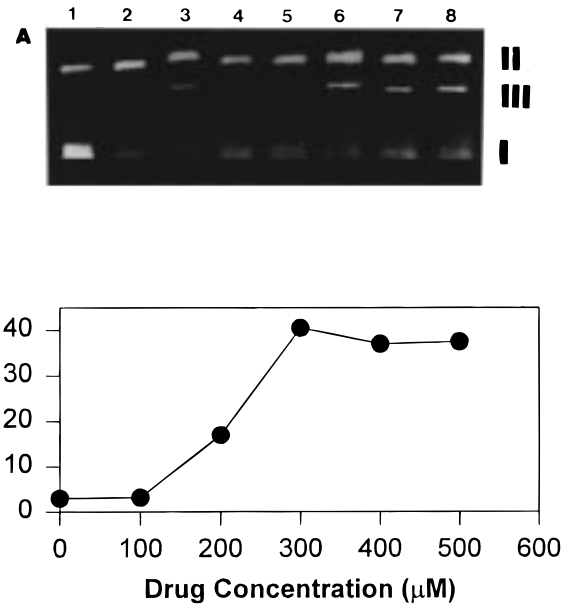

FIGURE 4: (A) The cleavage reaction was conducted by incubating pBR322 DNA (lane 1) with topo II (lane 2) in the presence of 100 μM m-AMSA (lane 3) and 100, 200, 300, 400, and 500 μM of RuBen (lanes 4−8). The positions of supercoiled, nicked circular, and linear (form 3) DNA are indicated by **I**, **II**, and **III**. (B) The plot shows the percentage of linear DNA formed with increasing concentrations of RuBen.

studied. The formation of the enzyme−drug−DNA complex can be seen by the appearance of linear DNA which results from DNA strand breaks caused by dissociation of the topo II homodimer by SDS (*29*). RuBen stabilized the enzyme−DNA cleavable complex at a concentration of 200 μM, as seen by the appearance of linear DNA equivalent to 17% of the total DNA. At 300 μM, the linear DNA increased to 40.5% and then decreased to ~37% for the higher drug concentrations (Figure 4). RuSal did not induce cleavage complex formation even at 500 μM concentration (data not shown).

Presence of Ruthenium and DNA in Cleavage Complex. The immunoprecipitation assay was performed to get a direct evidence for the involvement of RuBen in the drug-induced cleavage complex. The cleavage assay was conducted in the presence of 500 μM concentrations of the ruthenium drugs. After incubation, the enzyme in the cleavage complex as well as the free enzyme was immunoprecipitated with anti-topo II antibody. The antigen−antibody complex was then trapped in protein A agarose. Samples were washed to remove unbound components, and the bound enzyme was released from protein A agarose by 1% TCA and analyzed for the presence of ruthenium by atomic absorption spectroscopy. The results presented in Table 1A show that, while 46% of 500 μM RuBen is present in the cleavage complex, only 9% of RuSal is present in the same. Concentrations less than 2% (20 ng) could not be determined accurately by the instrument used and they were expressed as such.

Table 1: Presence of Ruthenium and DNA in Cleavage Complex[a]

	RuBen (%)	RuSal (%)
(A) Ruthenium		
DNA + Topo II	0	0
Drug	<2	<2
DNA + Drug	<2	<2
Topo II + Drug	8 ± 0.82	<2
DNA + Topo II + Drug	46 ± 3.05	9 ± 1.63
(B) DNA		
DNA + Topo II	3.0 ± 0.5	3.0 ± 0.5
DNA	0.5	0.5
DNA + Drug	1.0 ± 0.5	1 ± 0.7
Topo II + Drug	0	0
DNA + Topo II + Drug	21 ± 1.63	3 ± 0.82

[a] Data are presented as a percentage mean of three independent experiments conducted in triplicates, and standard deviations are given against each value.

The presence of DNA in the cleavage complex was confirmed by repeating the same assay in the presence of ^{3}H-labeled DNA. After TCA treatment, the products were spotted on filter paper strips and the radioactivity was measured. The results presented in Table 1B show that 21% of 0.6 μg of DNA is present in the RuBen-induced cleavage complex, as compared to 3% in the RuSal-induced complex. All of the controls correlate well with the atomic absorption spectral data. These results confirm the bidirectional interaction of RuBen with DNA and topo II. RuSal shows such a bidirectional binding to a very small extent.

Effect on ATPase Activity of Topoisomerase II. This assay was performed to examine the effect of ruthenium drugs on the ATPase activity of topo II. The relaxation assay was performed with increasing concentrations of the drugs in the presence of γ^{32}P ATP and products were resolved on PEI Cellulose-F TLC sheets. The results show that RuBen inhibited ATP hydrolysis in a dose-dependent manner. At 500 μM concentration, it could inhibit 50% of the total ATPase activity while RuSal could inhibit 13.5% of the ATPase activity (Figure 5).

Drug−DNA Interactions. The melting of calf thymus DNA was studied in the presence of increasing concentrations of drugs. The melting temperature curves showed a gradual increase in T_m with increasing concentrations of RuBen and RuSal (Figure 6A,B). Figure 6D shows that RuBen and RuSal exert a minor increase in the curve width of melting curves plotted against drug/nucleotide (D/N). The DNA intercalator m-AMSA, caused a major change in the curve width. In Figure 6C, D/N was plotted against the T_m values,

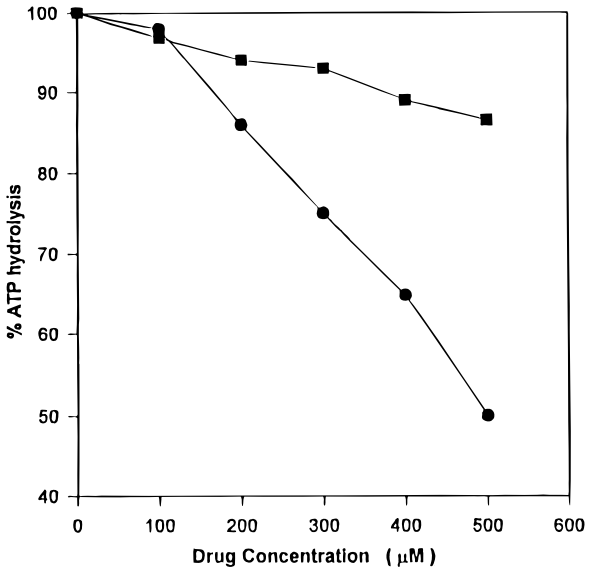

FIGURE 5: Inhibition of ATPase activity of topo II by RuBen (●) and RuSal (■). ATP hydrolysis in the control sample was taken as 100% and values in the presence of increasing concentration of the drugs are presented as mean of three experiments; data is plotted as the percentage of ATP hydrolyzed versus the concentration of drug in micromolar units.

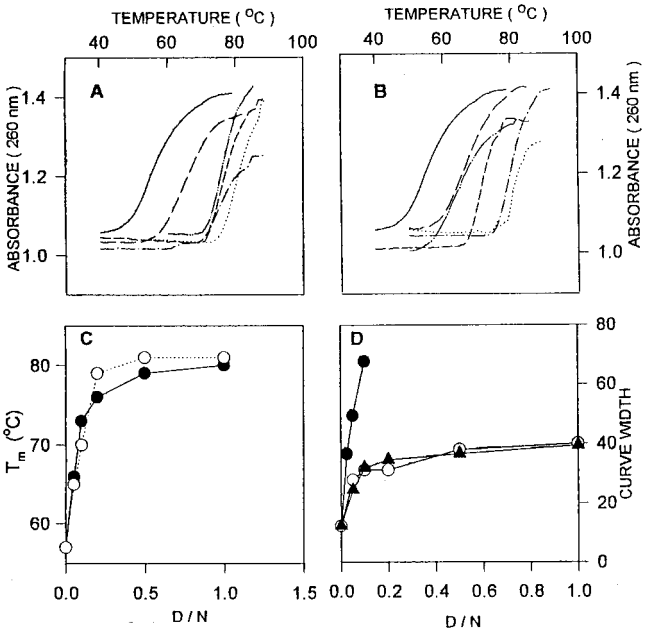

FIGURE 6: Drug−DNA-binding studies. (A) RuBen increases the T_m of calf thymus DNA from 57 °C for DNA control (—) to 66, 73, 76, 78, and 80 °C for DNA nucleotide-to-drug ratios of 20:1 (— — —), 10:1 (-···-), 5:1(- - -), 2:1(-·-), and 1:1 (···), respectively. (B) RuSal shows an increase in T_m of 65, 70, 79, 81, and 81 °C for the same drug to DNA ratios. (C) D/N (drug/nucleotide) plotted against the increase in T_m by RuBen (●) and RuSal (○) to determine specific drug binding to DNA nucleotides from the slopes of the curves. (D) D/N plotted against curve width shows a characteristic increase in curve width by m-AMSA (●) and a very small increase by RuBen (▲) and RuSal (○).

and the slopes of the curves were calculated to determine the stoichiometric binding of drug to DNA. RuBen showed a DNA-binding stoichiometry of 4 nucleotides and a weak binding stoichiometry of 7 nucleotides per drug molecule, while RuSal showed a stoichiometry of 4 nucleotides per molecule.

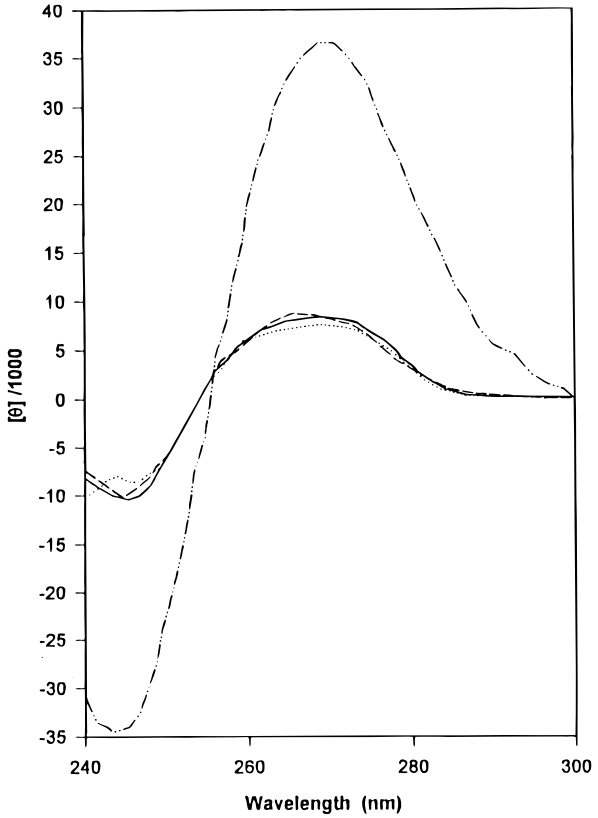

FIGURE 7: The circular dichroism spectra of pBR322 DNA (—) in the presence of RuBen(···) and RuSal(- - -) shows a small change in the molar ellipticity of DNA while m-AMSA(-···-) shows a very prominent change at a concentration less than 5 times that of the ruthenium drugs.

In the 1D and 2D gel mobility assays, it was observed that neither RuBen nor RuSal could change the DNA mobility or DNA conformation (data not shown).

Circular dichroic spectra of pBR322 DNA showed that RuBen and RuSal marginally affected the DNA conformation at the concentration which showed maximum inhibition of topo II relaxation activity. In comparison, m-AMSA caused a significant change in the DNA conformation (Figure 7).

DISCUSSION

Though DNA is implicated as the main target for anticancer ruthenium compounds (*30*), our data suggests that, apart from DNA, topo II poisoning may also be an effective mode of antineoplastic activity for one of the ruthenium compounds tested. We have compared an organometallic complex (Ruben) with a coordinated covalent complex (RuSal) for antiproliferative action and poisoning of topo II. Both compounds show good antiproliferative action; that of RuBen is 16% more than RuSal at the highest concentration tested. The relaxation, cleavage, and immunoprecipitation assays clearly show that RuBen can poison topo II through a drug-induced cleavage complex formation. RuSal, on the other hand, causes partial inhibition of relaxation activity and does not form a cleavage complex.

Analysis of the curve width of DNA melting curves is a useful way to distinguish between intercalative and external binding (*28*). Intercalators substantially increase the width of melting curves, while external binders have a smaller effect on this parameter. m-AMSA shows a curve width

typical of a DNA intercalator while RuBen and RuSal seem to fit into the group of compounds which bind externally to DNA like 2,2′-bipyridyl and terpyridyl complexes of ruthenium (*28*). Since both RuBen and RuSal show similar DNA binding, the metal atom in them may directly interact with DNA. The ruthenium atom could bind outside the DNA helix through ionic interactions or by covalent bonding with the nucleotide bases. In RuBen, an intercalative mode of DNA binding is not possible because the benzene ring forms an organometallic bond with the ruthenium atom, which prevents π-orbital stacking interaction of the aromatic ring with DNA bases. In RuSal, since there are no organometallic bonds, the π-stacking orbitals in the salicylaldoxime ligand are not affected. But the compound does not intercalate to DNA. Whether the orientation of the salicylaldoxime ligands or the presence of the metal atom absolve an intercalative mode of binding, it cannot be explained at present. RuBen and RuSal bind similarly to DNA but show different sensitivity for topo II poisoning. This points toward ligand involvement in topo II poisoning.

The strong DNA-binding ability of the ruthenium drugs prompted us to examine if these compounds produce conformational changes in DNA which could block enzyme activity. The gel mobility assays showed no change in DNA migration or conformation. This was confirmed by CD spectral analysis, which showed an inconsequential change in DNA conformation in the presence of RuBen and RuSal. Further, the ATPase assay shows that RuBen inhibits the DNA-stimulated ATPase activity of topo II. This is possible only if the drug induces the formation of the enzyme−drug−DNA cleavage complex or if the drug directly interacts with the enzyme at the ATPase domain. The first possibility seems true, which is supported by the cleavage reaction.

On the basis of molecular modeling analyses and superimposition of drug structures, a putative structure was proposed for topo II cleavage complex-forming drugs, which shows that these drugs have three distinct domains in them; the first is a planar ring system, the second is a pendant ring, and the third is a pendant moiety of heterogeneous structure (*31*). Though studies have shown that this structure is not an absolute requirement for topo II poisoning (*17*), most poisons do have large planar aromatic domains for DNA binding and substituents for enzyme interaction. It is interesting that a simple and small molecule like RuBen, with only one aromatic ring, could poison topo II by cleavage complex formation. RuBen has an octahedral geometry (*37*) which may facilitate the spatial orientation of its ligands to form interactions with enzyme. This interaction by the benzene, chloride, and DMSO ligands of RuBen may play an important role in poisoning the enzyme.

Prior to enzyme action, RuBen bound to DNA may interact with the catalytic domain of one or both monomers of topo II through the chloride atoms and the methyl groups of DMSO. The benzene ring may fit into some pocket in the enzyme and stearically hinder the conformation changes in the enzyme required for DNA religation. Whatever the mode of action, RuBen traps the cleaved DNA and topo II in the cleavage complex and prevents DNA religation action of the enzyme. The cleavage assay confirms that RuBen indeed shifts the enzyme's cleavage/religation equilibrium toward DNA cleavage.

In RuSal, the planar salicylaldoxime ligands are attached to the metal atom and oriented with an angle of ~40° to each other along the planar axis. This orientation may block enzyme action to a certain extent when the DNA-bound drug approaches the catalytic domain of topo II but may not allow a strong interaction with the enzyme. Even if an interaction does take place, the coordinated metal−ligand bonds may not provide a strong interface for cleavage complex formation. This could explain RuSal's ability to partially inhibit the relaxation activity of topo II, but not induce cleavage complex formation.

DNA intercalating topo II poisons intercalate to DNA through π-stacking interactions of their planar rings with DNA bases. The side chains of these drugs are involved in enzyme interaction. Such an interaction is important in facilitating the formation of the drug−enzyme−DNA ternary complex. Though RuBen binds externally to DNA nucleotides, it may still form a similar ternary complex in which the metal atom binds to DNA and ligands on the metal atom interact with topo II.

These findings allow us to propose a probable mode of topo II poisoning by RuBen. The metal atom interacts covalently or noncovalently with DNA nucleotides and the ligands form cross-links with the enzyme and prevent the DNA religation step, leading to the formation of a stable drug-induced cleavage complex, which is the hallmark of most topo II poisons. Such topo II poisons increase the steady state concentration of cleavage complexes which harbor topo II-associated double strand breaks. These become permanent double strand fractures following traversal by replication complexes. The accumulation of such DNA breaks in cells ultimately results in cell death by apoptosis or necrosis (*26*, *27*). RuBen could be categorized as a topo II poison which is a cleavable complex-forming, DNA-binding but nonintercalating agent.

Similar DNA interaction and effective antiproliferative action of RuBen and RuSal indicate that inhibition of the lymphoma cell proliferation may in part be due to a topo II-independent mechanism, probably at the DNA level. In RuSal, the salicylaldoxime ligand may also cause antiproliferative action. As an analogue of pyridoxal, salicylaldoxime is known to inhibit pyridoxal kinase activity and hinder transamination and decarboxylation processes leading to inhibition of protein synthesis, causing appreciable cytotoxicity (*28*). The marginally higher antiproliferation activity of RuBen in comparison with RuSal may possibly be due to topo II poisoning.

Studies indicate that antitumor activity of DNA-binding drugs in most cases depends on their capacity to interfere with catalytic activity of topo II (*25*, *27*). We have limited the scope of this work to topo II targeting, though ruthenium drugs, being DNA-binding agents, may interact with other DNA-binding proteins (e.g., DNA polymerases) and other biomolecules in the cell leading to toxicity generally associated with chemotherapy.

A better understanding of the molecular action of RuBen and the inherent advantage of ruthenium compounds (in lieu of their selectivity for entering tumor tissues) can aid in designing novel ruthenium compounds which poison topo II with higher potency and show substantial anticancer action, while mitigating the toxic side effects to a certain degree.

We have demonstrated, for the first time, topo II poisoning by a ruthenium compound and its relative antiproliferation activity.

ACKNOWLEDGMENT

We acknowledge CSIR for financial support. YNVG and DJ thank UGC and CSIR respectively for providing fellowships. We are thankful to Dr. M. Ramanadham for extending his laboratory facilities and for a thorough reading of the manuscript. We thank Ms. C. Subbalaxmi and the Director of CCMB for helping with the CD spectral analysis. We thank Dr. Robin Mukhopadhyaya of Cancer Research Institute, Mumbai, for the gift of Crit-2 cell line. We thank Bioinformatics center, I.I.Sc., Bangalore for providing the facility for molecular modeling.

SUPPORTING INFORMATION AVAILABLE

Characterization of ruthenium complexes and 1D and 2D gel mobility assays. This material is available free of charge via the Internet at http://pubs.acs.org.

REFERENCES

1. Wang, J. C. (1985) *Annu. Rev. Biochem. 54*, 665−697.
2. Watt, P. M., and Hickson, I. D. (1994) *Biochem. J. 303*, 681−695.
3. Holm, C. (1994) *Cell 77*, 955−957.
4. Hirano, T., and Mitchison, T. J. (1993) *J. Cell Biol. 120*, 601−612.
5. Earnshaw, W. C., and Heck, M. M. S. (1985) *J. Cell Biol. 100*, 1716−1725.
6. Earnshaw, W. C., Halligan, B., Cooke, C. A., Heck, M. M. S., and Liu, L. F. (1985) *J. Cell Biol. 100*, 1706−1715.
7. Gasser, S., and Laemmli, U. K. (1986) *EMBO J. 5*, 511−518.
8. Liu, L. F. (1989) *Annu. Rev. Biochem. 58*, 351−375.
9. Osheroff, N., Zechiedrich, E. L., and Gale, K. C. (1991) *BioEssays 13*, 269−275.
10. Roca, J. (1995) *Trends Biochem. Sci. 20*, 156−160.
11. Berger, J. M., Gamblin, S. J., Harrison, S. C., and Wang J. C. (1996) *Nature 937*, 225−232.
12. Zwellig, L. A. (1985) *Cancer Metastasis Rev. 4*, 263−276.
13. Glisson, B. S., and Ross, W. E. (1987) *Pharmacol. Ther. 32*, 89−106.
14. Pommier, Y., Capranico, G., Orr, A., and Kohn, K. W. (1991) *Nucleic Acids Res. 19*, 5973−5980.
15. Roca, J., and Wang, J. C. (1994) *Cell 77*, 609−616.
16. Robinson, M. J., and Osheroff, N. (1990) *Biochemistry 29*, 2511−2515.
17. Capranico, G., Palumbo, M., Tinelli, S., Mabilia, M., Pozzan, A., and Zunino, F. (1994) *J. Mol. Biol. 235*, 1218−1230.
18. Kopf-Maier, P. (1994) *Eur. J. Clin. Pharmacol. 147*, 1−16.
19. Haiduc, I., and Silvestru, C. *Organometallics in Cancer Chemotherapy*, Vol II, CRC Press LLC, FL.
20. Sava, G., Pacor, S., Bregant, F., and Ceschia, V. (1991) *Anticancer Res. 11*, 1103−1108.
21. Galande, S., and Muniyappa, K. (1996) *Biochim. Biophys. Acta 1308*, 58−66.
22. Bradford, M. M. (1976) *Anal. Biochem. 72*, 248−254.
23. Wang, Z., and Rossman, T. G., (1994) *BioTechniques 16*, 460−463.
24. Zelonka, R. A., and Baird, M. C. (1972) *Can. J. Chem. 50*, 3063−3072.
25. Lumme, P., and Elo, H. (1984) *Inorg. Chim. Acta 92*, 241−251.
26. Osheroff, N., Shelton, E. R., and Brutlag, D. L. (1983) *J. Biol. Chem. 208*, 9536−9543.
27. Zechiedrich, E. L., Christiansen, K., Anni, H., Ole, W., and Osheroff, N. (1989) *Biochem*istry *28*, 6229−6236.
28. Kelly, J. M., Tossi, A. B., McConnell, D. J., and OhUigin, C. (1985) *Nucleic Acids Res. 13*, 6017−6033.
29. Rene, B., Fosse, P., Khalifa, T., Alain, J., and Bailly, C. (1996) *Mol. Pharmacol. 49*, 343−350.
30. Clarke, M. J. (1989) *Prog. Clin. Biochem. Med. 10*, 25−39.
31. MacDonald, T. T., Lehnert, E. K., Loper, J. T., Chow, K. C., and Ross, W. E. (1991) *DNA Topoisomerases in Cancer* (Potmesil, M.; and Kohn, K. W., Eds.) pp 199−214, Oxford University Press, New York.
32. Froelich-Ammon, S. J., and Osheroff, N. (1995) *J. Biol. Chem. 270*, 21429−21432.
33. Chen, A. Y., and Liu, L. F. (1994) *Annu. Rev. Pharmacol. Toxicol. 34*, 191−218.
34. Martin, D. W., Jr. (1983) *Harper's Review of Biochemistry*, p 97, Lange Medical Pub., Los Altos, CA.
35. Vinter, J. G., Davis, A., and Saunders, M. R. (1987) *J. Comput.-Aided Mol. Des. 1*, 31−51.
36. Elschenbroich, Ch., and Salzer, A., (1992) *Organometallics − A Concise Introduction*, p 252−385, VCH Publications.
37. Bennet, M. A., and Smith, A. K., (1974) *J. Chem. Soc., Dalton Trans.* 233−241.

BI981990S